

Investigating the Potential of Tide- and Wind-Induced Currents for Renewable Energy in Northern Vietnam

Tuan Anh Le^{1,2} and Huu Nghi Tran³ (2025)

¹Faculty of Civil Engineering, Ho Chi Minh City University of Technology (HCMUT), Vietnam

²Vietnam National University, Ho Chi Minh City, Vietnam

³Power Engineering Consulting Joint Stock Company 2 (PECC2), Ho Chi Minh City, Vietnam

DOI: <https://doi.org/10.14796/JWMM.S541>

ABSTRACT

Renewable energy is increasingly recognized as the trend and future of sustainable societies. With a long coastline of 3,260 km and vast open sea areas, Vietnam has significant potential for clean energy development. This potential is not limited to wind power alone but extends to encompass a broader range of water-related energy sources. In this paper, the authors employ Delft3D software to create a comprehensive hydrodynamic model that investigates the potential of current velocities in Northern Vietnam, particularly the area surrounding Coto Island, influenced by both tidal variations and wind fields. The model's objective is to preliminarily estimate the potential area for tidal stream energy based on the average current speed. The analysis is guided by international technical criteria (EMEC 2009; IEC-TS 2015), which recommend a yearly average current speed exceeding 0.5 m/s. Preliminary findings highlight several promising locations north of Coto Island, where current speeds reach up to 1.2 m/s. Further in-depth research needs to be conducted, considering the development of tidal stream energy technologies, to explore suitable development plans for Vietnam.

1. INTRODUCTION

1.1 Background

Currently, tidal energy is utilized or investigated globally in three primary forms: tidal barrages (also known as tidal range) which utilize the potential energy of the tide, tidal currents (also known as tidal stream) which operate based on kinetic energy for the tide and combined tidal energy technologies.

Tidal barrage technology is one of the earliest and most cost-effective methods for generating 1 kWh of electricity (Boretti 2020), with the inaugural project commencing in France in 1966 (La

Le, T.A., and H.N. Tran. 2025. "Investigating the Potential of Tide- and Wind-Induced Currents for Renewable Energy in Northern Vietnam." *Journal of Water Management Modeling* 33: S541.

<https://doi.org/10.14796/JWMM.S541> www.chijournal.org ISSN: 2292-6062 ©Le and Tran 2025



Rance power station) (Charlier 2007). However, this technology has garnered limited attention due to its significant environmental impacts. According to Boretti 2020, the success of the tidal barrage in France has not been replicated in other locations when considering the environmental cost. For example, despite the UK possessing a substantial theoretical tidal energy potential of 120 TWh/year, no tidal barrage projects have been developed in the region (Petley et al. 2019).

To address these environmental concerns, tidal stream energy was proposed in 1981, receiving sustained investment starting in 2003, largely inspired by advancements in wind power technology. The International Renewable Energy Agency indicates that the current cost of generating 1 kWh of electricity from tidal stream is higher than from wind energy, but this cost is anticipated to decline in the near future (IRENA 2021).

The third method, which combined potential and kinetic energy, remains under investigation (IEA-OES 2021). Consequently, electricity generated by tidal stream (kinetic energy) is considered a prospective energy source for the future.

The potential for harnessing tidal power in the Vietnamese East Sea has been explored in numerous studies, focusing on both tidal range and tidal stream energy. The International Renewable Energy Agency (IRENA 2021) published a global tidal energy potential map based on tidal amplitude, identifying two key exploitable areas in Vietnam: Thanh Hoa to Quang Ninh and Vung Tau to Ca Mau. Additionally, a 2022 study by Do and colleagues from the National University analyzed tidal amplitudes at eight regions along Vietnam's coast. They highlighted the Gulf of Tonkin as having significant tidal power potential, with an estimated capacity of 17.33 GWh/km²/year (Do et al. 2022). Another study by Vu (2017) assessed tidal energy potential in 49 coastal bays in Vietnam, identifying Ha Long Bay and Ganh Rai Bay as promising areas with theoretical potentials of 4.73 TWh and 0.71 TWh, respectively.

Regarding tidal stream power, Zheng et al. 2015 estimated that the potential energy in the South China Sea could reach 0.4 GW. Furthermore, another study by Quirapas and Taeihagh (2020) assessed the potential for wave energy, tidal stream energy, and marine geothermal energy in the Asia-Pacific region, estimating that Vietnam has a tidal stream energy potential of 200–500 MW.

To assess tidal energy potential, most researchers rely on numerical modeling methods, while some use long-term water level measurements (Do et al. 2022). However, most tidal energy studies in Vietnam have focused on tidal range energy, which comes with certain limitations, whereas research on kinetic energy related to current speed remains limited. This study addresses this gap by analyzing current velocity regimes to identify the potential areas and estimate energy capacity.

2. METHODOLOGY

Several methods exist for investigating tidal currents. One approach involves analyzing observed data to evaluate the magnitude of current speed. However, this method heavily depends on the limited number of observation stations and can only estimate current speed at those specific locations, making it inadequate for identifying potential areas more broadly.

An alternative method uses numerical models calibrated with observed data. This method overcomes the limitations of the first approach by enabling the estimation of tidal stream power over larger areas around the observation stations (Wei et al. 2013; Lin et al. 2017). Previous study conducted by Tran et al. 2023 has applied numerical models to investigate the current fields in Vietnam, focusing on the northern Gulf of Tonkin and the southeastern coast. However, these studies excluded wind effects during simulations, and typically analyze only short periods, such as one month, which limits its ability to provide reliable yearly averages.

In this study, the authors utilized the numerical model Delft3D-FLOW to simulate the hydrodynamic regime within the computational area. The model, driven by both tidal forces and wind, generated results that include the current velocity field. Calibration and validation were performed by comparing the model outputs with measured data. Using the validated model, simulations were run for scenarios representing a typical year. Based on the resulting current speed data, the tidal stream power in the investigated areas was estimated using formulas from established technical guidelines, such as EMEC 2009 and IEC-TS 2015. The following sections detail the configuration of the numerical model, and the methodology used to estimate tidal kinetic energy from the simulated results.

The main equations used in Delft3D-FLOW are described in the next section. FLOW solves the continuity (Equation 1) and Navier–Stokes equations (Equation 2 and 3) for an incompressible fluid under shallow water and hydrostatic assumptions. Although the Delft3D-FLOW module can be applied to three-dimensional phenomena, we used a two-dimensional horizontal grid, establishing a shallow-water wave model, which is commonly used to simulate long waves such as storm surges, tsunamis, and tidal propagation (Takagi et al. 2019).

$$\frac{\partial \zeta}{\partial t} + \frac{1}{\sqrt{G_{\xi\xi}\sqrt{G_{\eta\eta}}}} \frac{\partial [(d+\zeta)U\sqrt{G_{\eta\eta}}]}{\partial \xi} + \frac{1}{\sqrt{G_{\xi\xi}\sqrt{G_{\eta\eta}}}} \frac{\partial [(d+\zeta)V\sqrt{G_{\xi\xi}}]}{\partial \eta} = Q \quad (1)$$

$$\begin{aligned} \frac{\partial u}{\partial t} + \frac{u}{\sqrt{G_{\xi\xi}}} \frac{\partial u}{\partial \xi} + \frac{v}{\sqrt{G_{\xi\xi}}} \frac{\partial u}{\partial \eta} + \frac{\varpi}{d+\zeta} \frac{\partial u}{\partial \sigma} - \frac{v^2}{\sqrt{G_{\xi\xi}\sqrt{G_{\eta\eta}}}} \frac{\partial \sqrt{G_{\eta\eta}}}{\partial \xi} \\ + \frac{uv}{\sqrt{G_{\xi\xi}\sqrt{G_{\eta\eta}}}} \frac{\partial \sqrt{G_{\xi\xi}}}{\partial \eta} - fv = -\frac{1}{\rho_0\sqrt{G_{\xi\xi}}} P_\xi + F_\xi + \frac{1}{(d+\zeta)^2} \frac{\partial}{\partial \sigma} \left(\nu_V \frac{\partial u}{\partial \sigma} \right) + M_\xi \end{aligned} \quad (2)$$

$$\begin{aligned} \frac{\partial v}{\partial t} + \frac{u}{\sqrt{G_{\xi\xi}}} \frac{\partial v}{\partial \xi} + \frac{v}{\sqrt{G_{\xi\xi}}} \frac{\partial v}{\partial \eta} + \frac{\varpi}{d+\zeta} \frac{\partial v}{\partial \sigma} + \frac{uv}{\sqrt{G_{\xi\xi}\sqrt{G_{\eta\eta}}}} \frac{\partial \sqrt{G_{\eta\eta}}}{\partial \xi} \\ - \frac{u^2}{\sqrt{G_{\xi\xi}\sqrt{G_{\eta\eta}}}} \frac{\partial \sqrt{G_{\xi\xi}}}{\partial \eta} + fu = -\frac{1}{\rho_0\sqrt{G_{\eta\eta}}} P_\eta + F_\eta + \frac{1}{(d+\zeta)^2} \frac{\partial}{\partial \sigma} \left(\nu_V \frac{\partial v}{\partial \sigma} \right) + M_\eta \end{aligned} \quad (3)$$

Where:

- ζ = free surface elevation above the reference plane (at $z = 0$),
- z = vertical coordinate in physical space,
- t = time,

- $G_{\xi\xi}, G_{\eta\eta}$ = coefficient used to transform curvilinear to rectangular coordinates,
- d = depth below the reference plane,
- ξ, η = horizontal, curvilinear coordinates,
- U = depth-averaged velocity in ξ -direction,
- V = depth-averaged velocity in η -direction,
- Q = contributions per unit area due to the discharge or withdrawal of water, precipitation, and evaporation,
- u = flow velocity in the x - or ξ -direction,
- v = fluid velocity in the y - or η -direction,
- σ = scaled vertical coordinate; $\sigma = (z - \zeta) / (d + \zeta)$,
- ω = vertical velocity relative to the moving σ -plane,
- f_u, f_v = Coriolis parameter (inertial frequency),
- ρ_0 = reference density of water,
- F_ξ, F_η = forces in the momentum equations represent the unbalance of horizontal Reynold's stresses,
- ν_v = vertical eddy viscosity coefficient,
- M_ξ, M_η = effects of external sources or sinks of momentum in ξ - and η -direction, including external forces by hydraulic structures, discharge, or withdrawal of water, wave stresses, etc., and
- P_ξ, P_η = pressure gradients.

2.1 Computational domain

According to the literature, potential areas for tidal energy could be the northern Gulf of Tonkin and the southeastern coast. For instance, a study was conducted using the MIKE 21/3 model to investigate the effects of current and wave action on sediment transportation around Coto Island, located in the northern Gulf of Tonkin (Vu et al. 2013). They found that the predominant current velocity reached 0.6 m/s, and in some locations between islands, it could exceed 1 m/s, but the specific locations are not shown because that was beyond the goals of the study.

Therefore, in this study, the authors chose the area around Coto Island, which has shown high current speeds, to investigate the spatial distribution of tidal stream energy in detail. The study area covers the Gulf of Tonkin (Figure 1), within the range from latitude 18.7°N to 22.5°N, and longitude 105.5°E to 109°E, with a resolution of 0.02 degrees (~2 km). For the area of interest around Coto Island, the resolution is locally refined to 0.01 degrees (~1 km) (Figure 2).

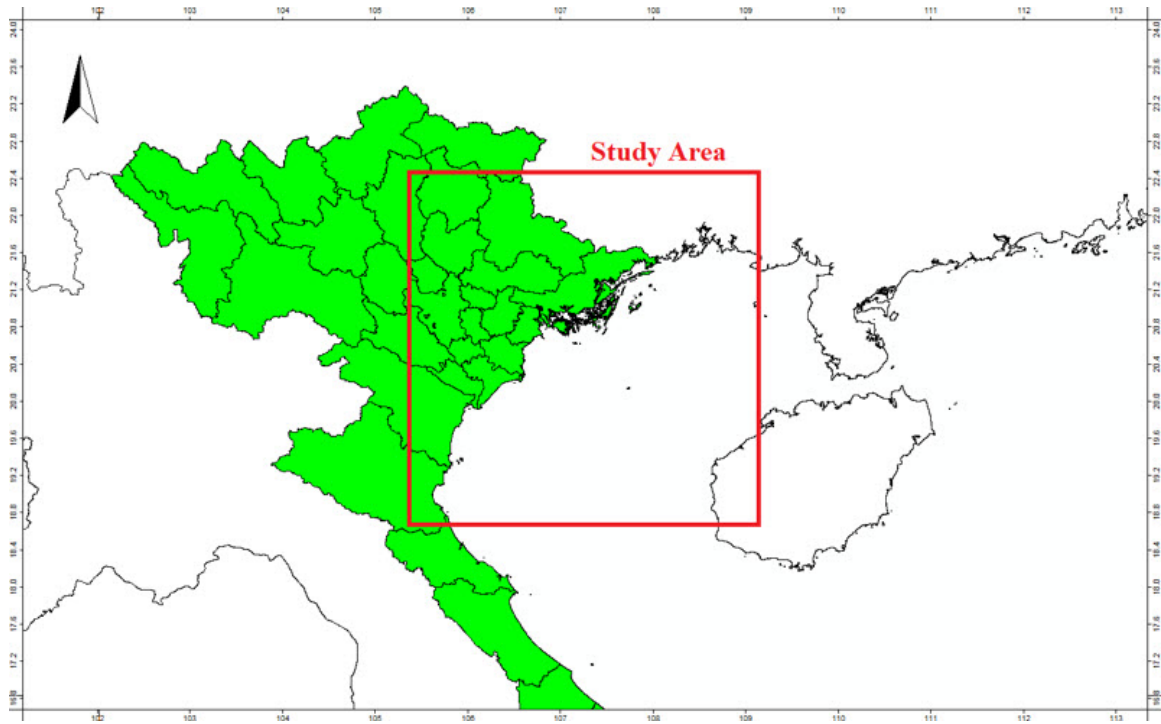


Figure 1 Study area.

2.2 Setting up the model

Along the two open boundaries, tidal forces are assigned. Each tidal constituent includes amplitude and phase values assigned to the start and end points of each boundary of the computational grid, retrieved from the global tide model TPXO. The bathymetry data is sourced from GEBCO 8 (Figure 3). The wind field, including x-direction and y-direction wind components and air pressure, is obtained from ECMWF.

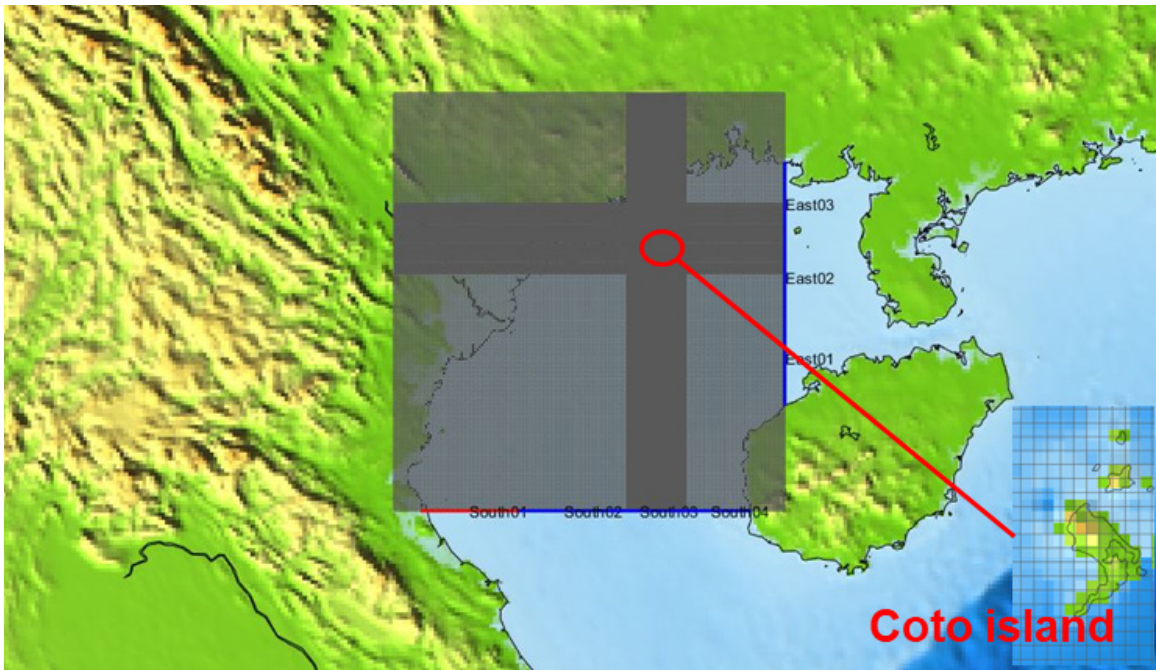


Figure 2 Computational domain.

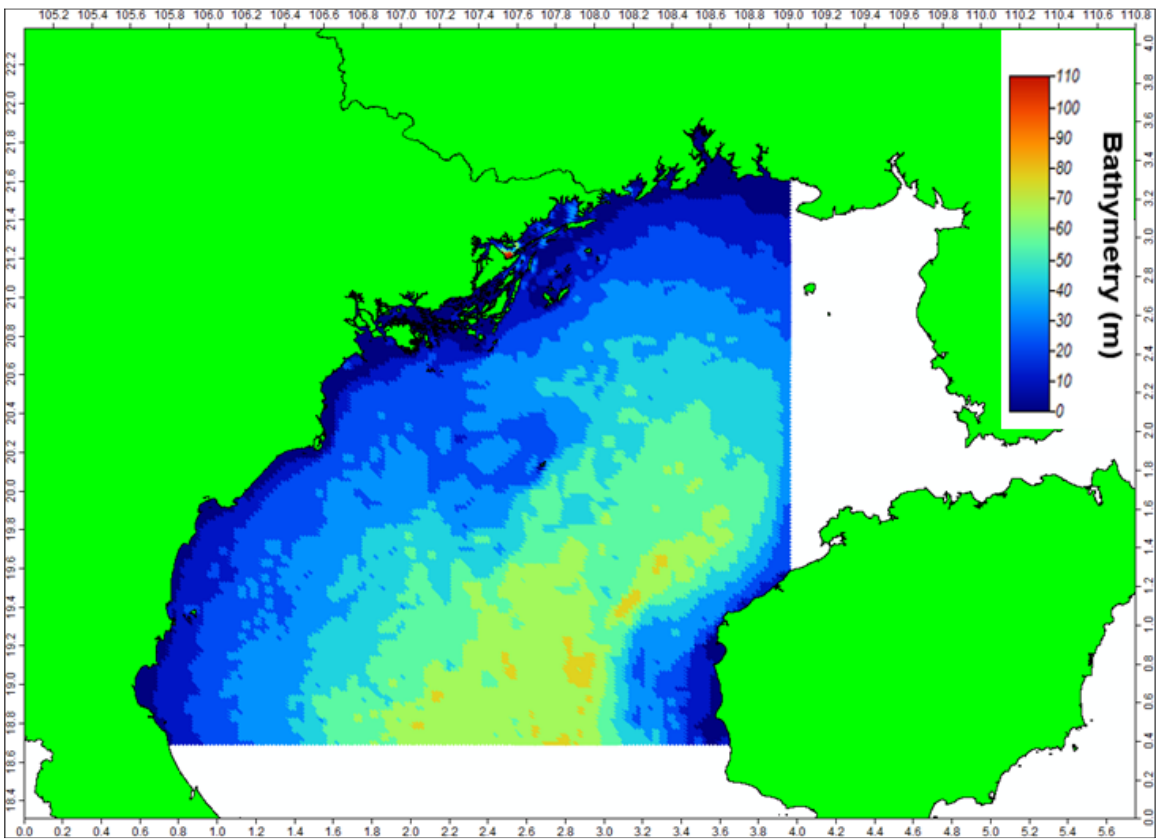


Figure 3 Bathymetric data.

2.3 Calibration and validation model

The primary driving force for coastal currents is the variation in water levels caused by tides. The key parameter that directly affects water levels and indirectly influences velocity is Manning's coefficient. According to a recent publication (Tran et al. 2023), a Manning's coefficient of 0.04 is suitable for the North Vietnam area. Therefore, in the first step, a value of 0.04 is applied to assess its appropriateness. There are two main wind seasons in this area: the Northeast monsoon season (corresponding to the dry season, from November to April) and the Southwest monsoon season (corresponding to the rainy season, typically from May to late September, or early October). The periods of January and October 2018 were chosen for water level calibration and validation, respectively, with data from the Hon Dau station (106°49'E 20°40'N), while the measured data in the neighboring area in May 2011 from the JICA study (JICA 2013) (stations C3, C4, C6) was used for checking the accuracy of simulated current speed due to the limited availability of measured data in this area (Figure 4). The criteria for RMSE and BIAS were considered based on the recommendation from Williams and Esteves (2017). Figure 5(a) presents time series plots comparing the model results with real data for both calibration (January 2018) and validation (October 2018), while Figure 5(b) illustrates the correlation between these two datasets for the same periods. According to the values of BIAS, RMSE (Figure 5(a)) and Correlation coefficient (Figure 5(b)), the simulated water level at Hon Dau station during the simulated period in January (calibration) and October 2018 (validation) fits well with the observed data, therefore confirming the suitability of choosing the Manning's coefficient for modeling.

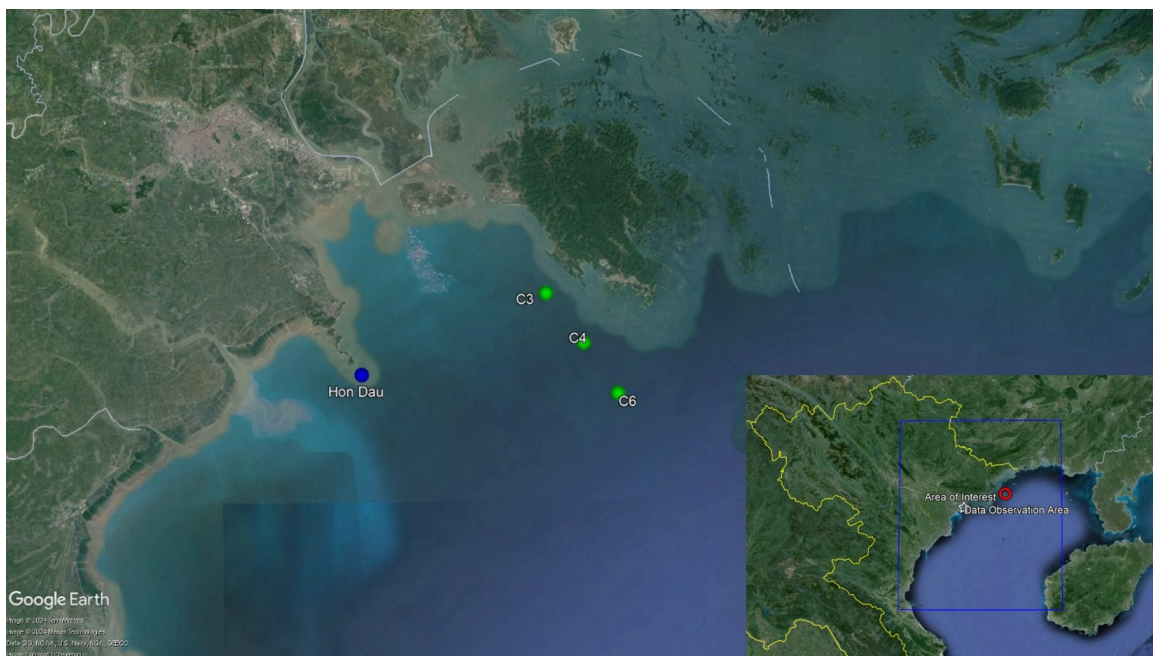
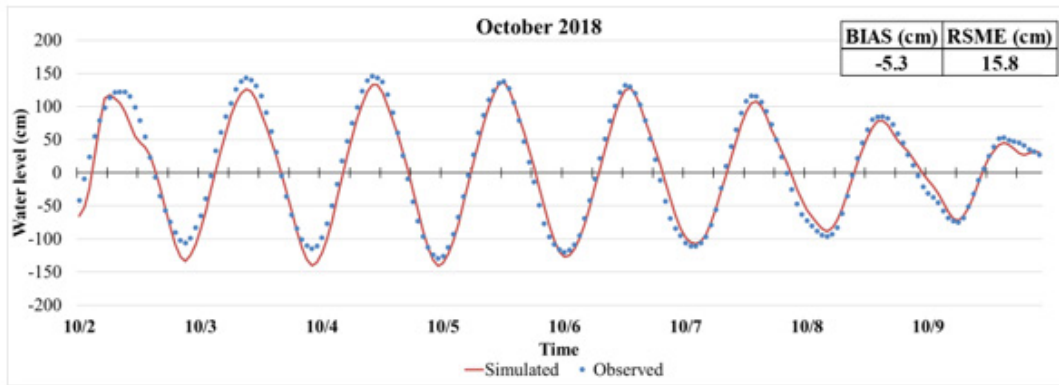
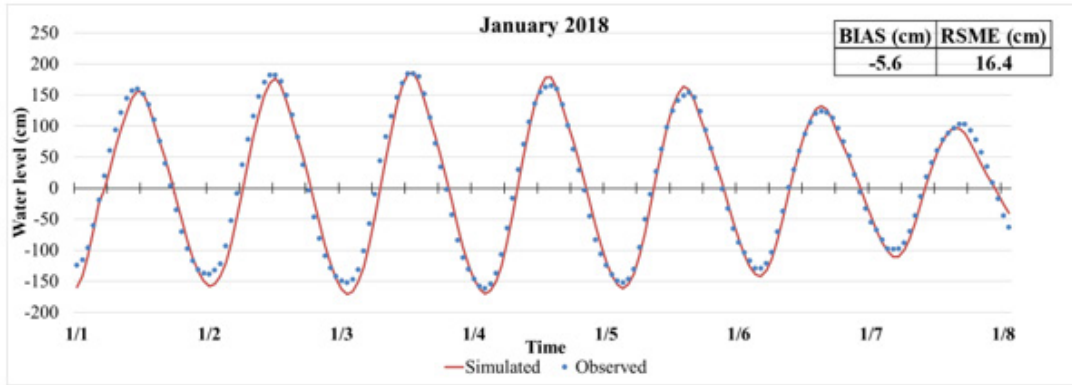
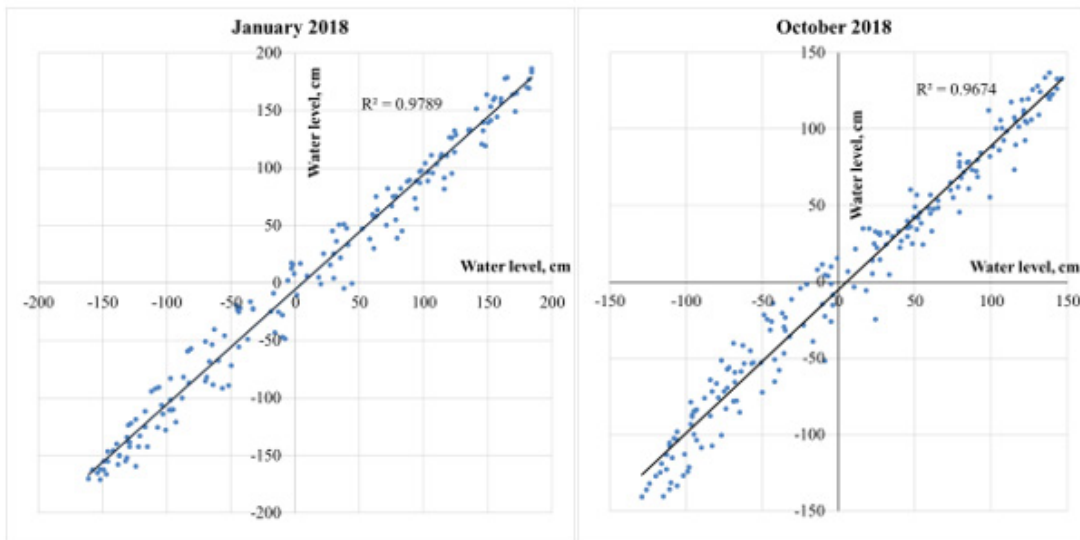


Figure 4 Water level (blue), and current speed (green) observation stations.



(a)



(b)

Figure 5 (a) Time series plots comparing model results with real data for both calibration (January 2018) and validation (October 2018) at Hon Dau station; and (b) illustrates the correlation between these two datasets for the same periods.

NOTE: Recommended from Williams and Esteves 2017. For water level: RMSE 10-15% of measured level range, BIAS less than 10 cm; $R > 0.95$.

The simulated current speed at C3, C4, and C6 (Figure 6) was underestimated compared to the measured data. In this study, only tidal force and wind force are applied, whereas the measured data in the field are also affected by waves. However, the gap is still acceptable (based on the recommendation from Williams and Esteves 2017), as shown in Table 1. After the validation process, the model is applied to run for the entire typical year of 2019 for the yearly average potential energy estimation. The yearly wind speed variation used as the environmental force is illustrated in Figure 7.

Table 1 Calibration and validation current speed results during May 2011 at stations from JICA’s study.

Station	Coordinates		Max. (m/s)	Mean (m/s)
	Longitude	Latitude		
C3	106°57’53.683”	20°43’27.104”	0.42 (0.59)	0.17 (0.15)
C4	106°59’52.058”	20°41’15.780”	0.21 (0.32)	0.09 (0.12)
C6	107°01’32.404”	20°38’53.106”	0.23 (0.43)	0.10 (0.16)

NOTE: The value in parentheses is from the JICA study. Williams and Esteves 2017 recommends that level performance for peak current speed should be within the range 0.05 – 0.2 m/s.

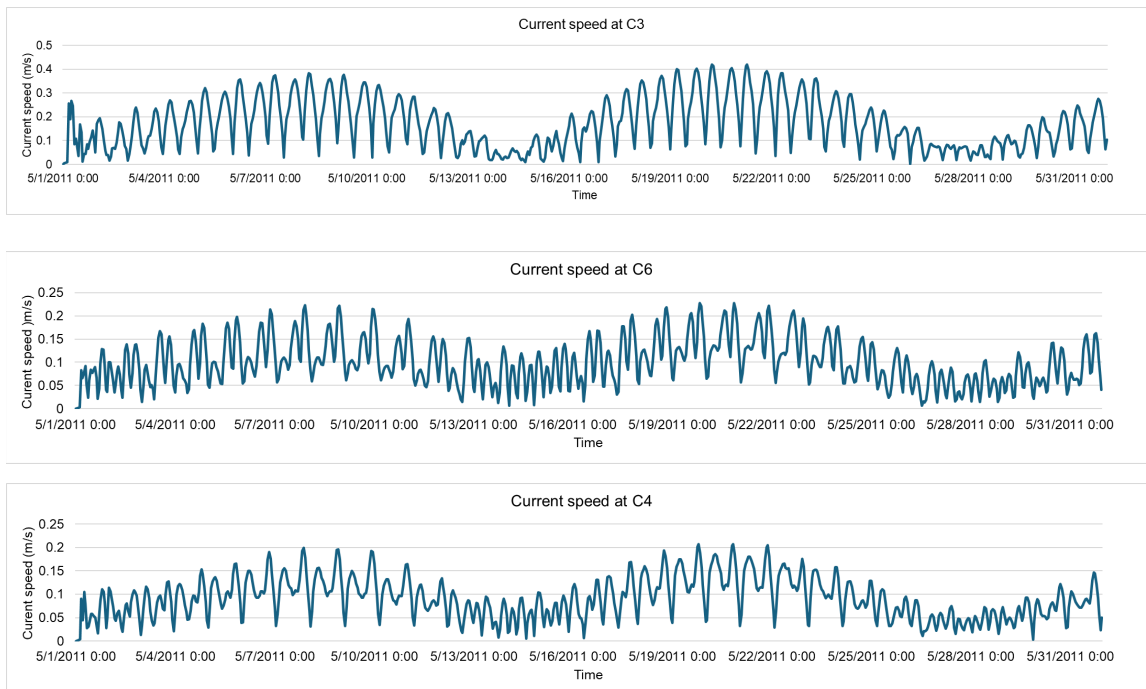


Figure 6 Simulated current speed at stations C3, C4, and C6.

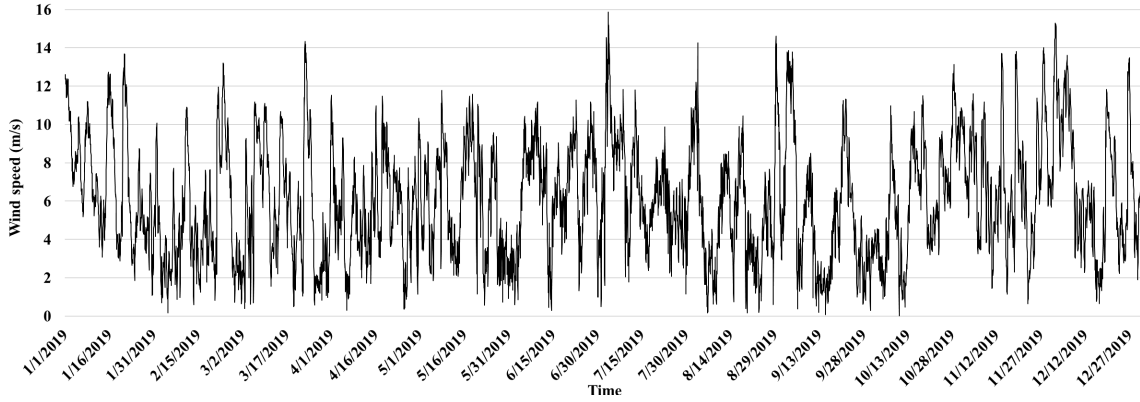


Figure 7 Yearly time-series wind speed at location 108°00'E 20°45'N.

2.4 Estimation of potential energy

According to the European Marine Energy Centre (EMEC 2009), an area is considered potential if its yearly-averaged velocity exceeds 0.5 m/s. Similarly, the technical guidelines IEC-TS 62600-201 (2015) indicate that in cases where the specific turbine technology has not been determined, the cut-in speed (V_{cut-in})—the speed at which a turbine starts rotating—is also 0.5 m/s. However, this threshold may be too strict for regions like the Northern Gulf of Tonkin, which has a tidal amplitude of around 3 m. Therefore, as a preliminary step, areas with current speeds slightly below 0.5 m/s are also deemed acceptable for further investigation.

Based on the preliminary results, several potential sites were identified by analyzing areas with the highest observed velocities. Potential areas were defined using criteria that specify sizes ranging from 1 km² (grid resolution 0.01° x 0.01° ~ 1 km x 1 km) to 2 km² (grid resolution 0.01° x 0.02° ~ 1 km x 2 km). The time series data of depth-averaged velocity for points (grid cells) within the potential sites were extracted from the model results. These values were then used to calculate the yearly average velocity at each site. The theoretical kinetic power density was calculated using the "Energy Flux Method" from EMEC 2009 (Equation 4):

$$P_{ij} = 0.5 \cdot \rho \cdot [\Sigma V_{ij}^3 / N] \quad (4)$$

Where:

- P_{ij} = yearly averaged kinetic power density (W/m²) at grid j ,
- ρ = seawater density (1,025 kg/m³),
- V_{ij} = time series velocity at different grid positions (m/s), and
- N = number time series velocity value in the investigated period, in this study, 1 year.

Then, the potential kinetic power (also referred as "average kinetic power flux" in EMEC 2009) is calculated:

$$Kinetic\ power\ (kW) = P_{ij} \cdot d_{cell} \cdot W_{cell} \quad (5)$$

Where:

- d_{cell} = depth at the grid cell, and
- W_{cell} = width of the grid cell (1,000 m).

3. RESULTS

Potential areas, consisting of multiple grid cells, were assessed based on the temporal and spatial distribution of current speeds (Figure 7). An area was considered to have potential if high current speeds—approximately 0.5 m/s or higher—were frequently observed. At this preliminary stage, no specific criteria for occurrence frequency were applied; instead, the selection process was carried out intuitively. Based on the numerical results, five potential sites with the most frequent high current speeds were *preliminarily* identified and labeled as Area 1, Area 2, Area 3, Area 4, and Area 5, as shown in Figure 8. The grid cell with the highest current speed in each area was then plotted (Figure 9). While current velocities exceeding 0.5 m/s also occur around the Coto Islands, the frequency is less significant compared to those in the five potential areas, where estimated velocities range from 0.6 m/s to over 1.2 m/s.

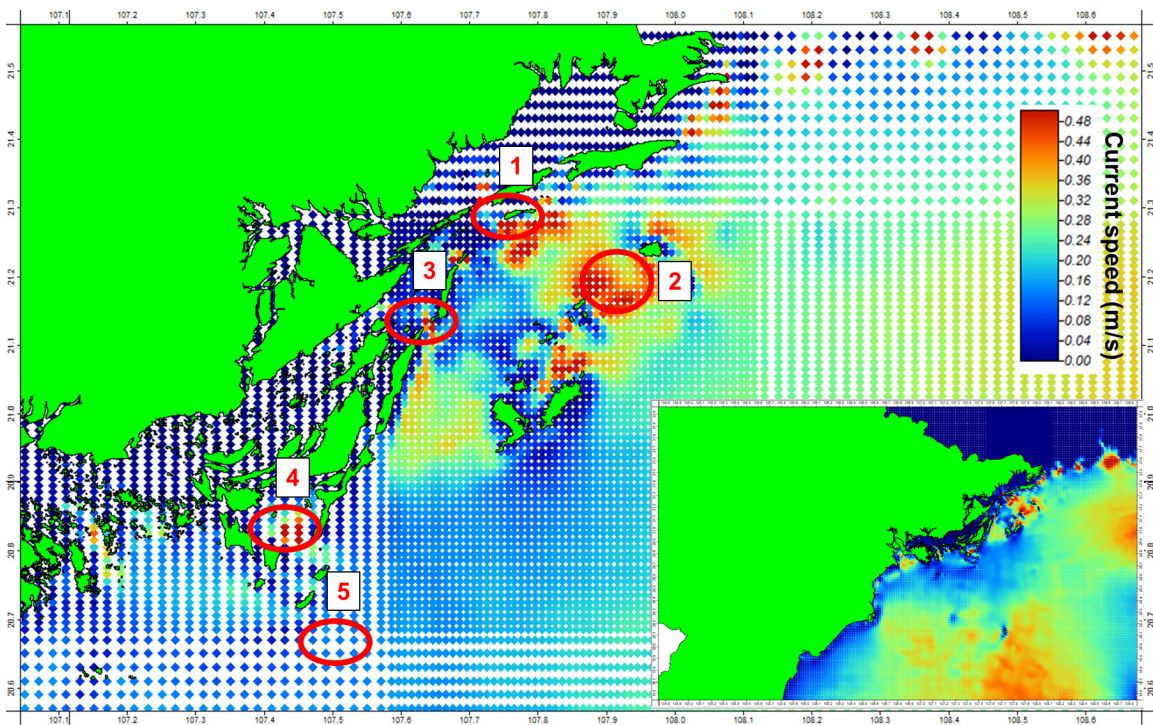


Figure 8 Spatial distribution of current speeds exceeding 0.5 m/s (shown in red) during the typical time step within the study area.

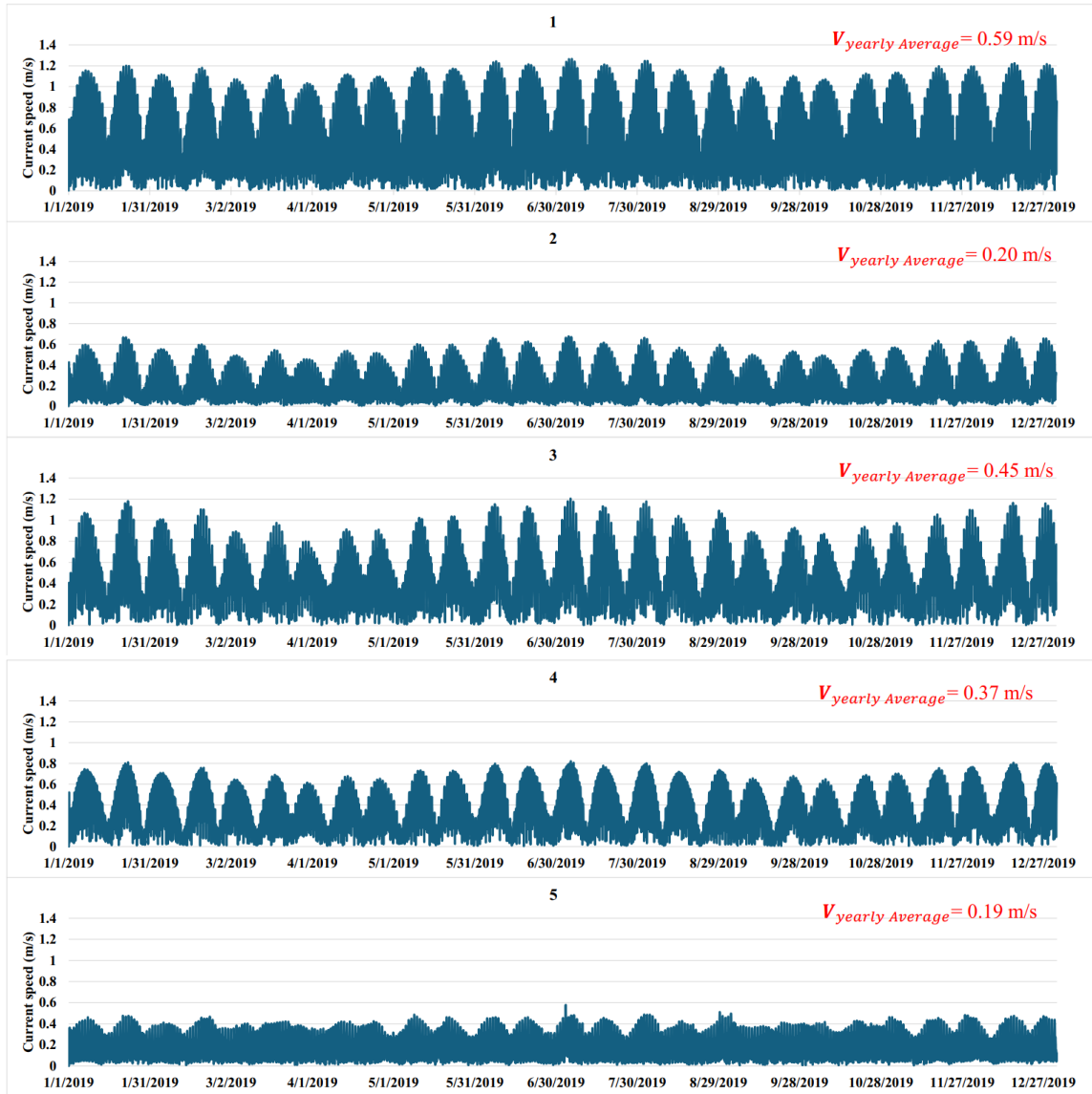


Figure 9 Plots of current speeds at potential areas.

4. DISCUSSION

Based on the EMEC 2009 criterion requiring a yearly average speed exceeding 0.5 m/s, Areas 1 and 3 have been shortlisted as potential sites. The theoretical kinetic power is estimated at 1,677 kW for Area 1, and 694 kW for Area 3, respectively (Table 2). The kinetic power results in this table were calculated using Equation 5.

Table 2 Calculation results of kinematic power in the potential areas.

Area	P_{ij} (W/m ²)	Depth (m)	Width (m)	Kinetic Power (kW)
Area 1 (grid cell)	201.07	8.34	1,000	1,677
Area 3 (grid cell)	85.78	8.10	1,000	694

According to the technical guidelines IEC-TS 62600-201, an important factor besides the cut-in speed (V_{cut-in})—the speed at which the turbine starts rotating—is the rated speed (V_{rated}), at which the turbine reaches its design power. The rated speed is defined as 71% of the maximum flow speed (V_{msp}) of the tidal current in the dataset. Based on our statistics, the V_{msp} for Areas 1 and 3 are 1.27 m/s and 1.21 m/s, respectively. Therefore, the corresponding V_{rated} values for these areas are 0.9 m/s and 0.86 m/s.

When we compare the V_{rated} values with the velocity exceedance frequency distributions of the two areas, we find that speeds exceeding V_{rated} occur approximately 22% of the time in Area 1, and 6% of the time in Area 3 (see Figure 10). This means that these higher speeds are present for 22% and 6% of the year, respectively. This information indicates that the potential for tidal current resources in Vietnam is very promising.

According to Equations 4 and 5, the kinetic power varies significantly depending on the current speed and water depth. In this study, the water depth is estimated based on the mean sea level. According to EMEC 2009, the grid cell size can affect peak velocities, introducing up to a 20% error. For the detailed investigation stage, the grid resolution should be finer than 500 m, or even finer than 50 m during the site assessment full-feasibility stage. In further detailed steps, a model that accounts for high-resolution grids and temporal as well as spatial fluctuations of water levels should be considered to more accurately estimate the kinetic power. In this study, the potential power of a single water area equivalent to 1 km² has been estimated. For exploitation purposes —such as establishing a farm with a power capacity higher than 3 MW— further investigation is needed. To accomplish this, the combination of numerical modeling and GIS technology should be applied to assess the potential of a larger area.

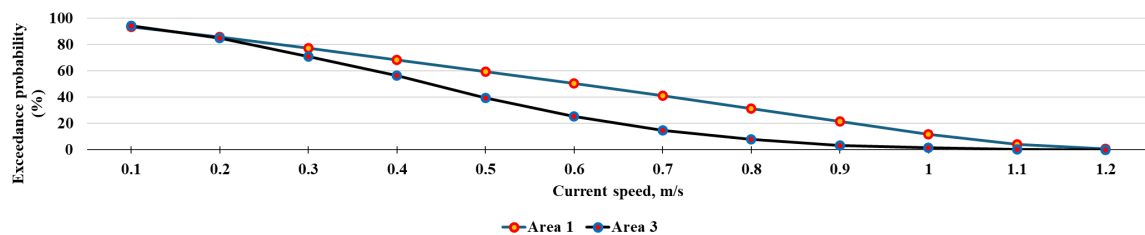


Figure 10 Exceedance probability of current velocity.

Future research should prioritize determining turbine technologies to suit the moderate flow velocities and the local water depth in the Gulf of Tonkin. This includes testing small-scale prototypes and assessing their performance under local conditions. Additionally, a detailed economic feasibility analysis is essential to evaluate the cost-effectiveness of tidal stream energy farms, considering installation, maintenance, and energy production costs, and comparing these with other renewable energy sources such as offshore wind. Environmental impact assessments should also be conducted to understand the ecological effects of turbine deployment on marine

ecosystems, sediment transport, and water quality. These steps will help advance the successful deployment of tidal stream energy in Vietnam, while contributing to the country's broader renewable energy goals.

5. CONCLUSION

This study focuses on investigating the tidal stream potential energy in the Gulf of Tonkin, especially around Coto Island, by implementing a numerical model. Both tidal and wind forces are considered as environmental factors. The simulated results reveal several promising areas, mainly around the small island to the north of Coto Island. The maximum current speed in the potential area exceeds 1.2 m/s, indicating a promising possibility for tidal stream potential with theoretical power of 1 km² water area reaching 1,667 kW. However, this study represents a preliminary step in evaluating tidal energy potential, as many additional criteria need to be considered. Further research is essential to determine the most suitable technologies for the local tidal conditions and water depths. The future roadmap should include field testing, detailed cost estimation, and comprehensive environmental impact assessments to ensure the successful deployment of tidal stream energy in Vietnam.

ACKNOWLEDGMENTS

We acknowledge Ho Chi Minh City University of Technology (HCMUT), and VNU-HCM for supporting this study.

REFERENCES

- Boretti, A. 2020. "Trends in tidal power development." *E3S Web of Conferences* 173, 01003. <https://doi.org/10.1051/e3sconf/202017301003>
- Charlier, H.R. 2007. "Forty candles for the Rance River TPP tides provide renewable and sustainable power generation." *Renewable and Sustainable Energy Reviews* 11 (9): 2032–2057. <https://doi.org/10.1016/j.rser.2006.03.015>
- Do, H.T., T.B. Nguyen, and T.M. Ly. 2022. "Tidal energy potential in coastal Vietnam." *Vietnam Journal of Science, Technology and Engineering* 64 (1): 85–89. [https://doi.org/10.31276/VJSTE.64\(1\).85-89](https://doi.org/10.31276/VJSTE.64(1).85-89)
- European Marine Energy Centre (EMEC). 2009. "Assessment of Tidal Energy Resource." Available online: https://www.emec.org.uk/?wpfb_dl=35
- IEA-OES. 2021. "Tidal current energy developments highlights. Technology Collaboration Programme." Available online: <https://www.ocean-energy-systems.org/publications/oes-brochures/document/tidal-current-energy-developments-highlights/>
- IEC Technical Specification 62600-201 (IEC-TS). 2015 "Marine energy – Wave, tidal and other water current converters – Part 201: Tidal energy resource assessment and characterization." Available online: <https://webstore.iec.ch/en/publication/22099>
- IRENA. 2021. "Offshore Renewables-An action agenda for deployment. G20-ITALIA." Available online: <https://www.irena.org/Publications/2021/Jul/Offshore-Renewables-An-Action-Agenda-for-Deployment>

- Japan International Cooperation Agency (JICA). 2013. "The detailed design study of Lach Huyen port infrastructure construction project. Final report on port portion of the project." Available online: https://openjicareport.jica.go.jp/pdf/12125332_01.pdf
- Lin, J., B. Lin, J. Sun, and Y. Chen. 2017. "Numerical model simulation of island-headland induced eddies in a site for tidal current energy extraction." *Renewable Energy* 101: 204–213. <https://doi.org/10.1016/j.renene.2016.08.055>
- Petley, S., D. Starr, L. Parish, Z. Underwood, and G.A. Aggidis. 2019. "Opportunities for tidal range projects beyond energy generation: Using Mersey barrage as a case study." *Frontiers of Architectural Research* 8 (4): 620–633. <https://doi.org/10.1016/j.foar.2019.08.002>
- Quirapas, M.A.J.R., and A. Taeihagh. 2020. "Ocean renewable energy development in Southeast Asia: Opportunities, risks and unintended consequences." *Renewable and Sustainable Energy Reviews* 137, 110403. <https://doi.org/10.1016/j.rser.2020.110403>
- Takagi, H., M.B. Pratama, S. Kurobe, M. Esteban, R. Aránguiz, and B. Ke. 2019. "Analysis of generation and arrival time of landslide tsunami to Palu City due to the 2018 Sulawesi earthquake." *Landslides* 16 (5): 983–991. <https://doi.org/10.1007/s10346-019-01166-y>
- Tran, N.H., A.T. Le, Q.T. Nguyen, H.H. Tran, and P.Q. Tran. 2023. "Tidal Current Energy Resource Assessment for Vietnam." *2023 Asia Meeting on Environment and Electrical Engineering (EEE-AM)*, Hanoi, Vietnam, 1–6. <https://doi.org/10.1109/EEE-AM58328.2023.10395159>
- Vu, H.D., H.L. Nguyen, N.T. Nguyen, N.T. Do, and T.T. Nguyen. 2013. "Study of Hydro-Dynamic characteristics during the Northeast Monsoon in the Co To area using the MIKE 21/3 FM model." *Journal of Hydro-Meteorology* 10, 2013. (in Vietnamese) Available online: <http://tapchikttv.vn/article/852>
- Vu, H.H. 2017. "Vietnam marine energy: Potential and proposed appropriate extraction technologies." *Journal of Science and Technology in Civil Engineering (JSTCE)* 4 (1): 81–92. (In Vietnamese) Available online: <https://stce.huce.edu.vn/index.php/vn/article/view/914>
- Wei, B.C., C.L. Wen, and H.H. Ming. 2013. "Modeling assessment of tidal current energy at Kinmen Island, Taiwan." *Renewable Energy* 50: 1073–1082. <https://doi.org/10.1016/j.renene.2012.08.080>
- Williams, J.J., and L.S. Esteves. 2017. "Guidance on setup, calibration, and validation of hydrodynamic, wave, and sediment models for shelf seas and estuaries." *Advances in Civil Engineering* 2017, 251902. <https://doi.org/10.1155/2017/5251902>
- Zheng, J., P. Dai, and J. Zhang. 2015. "Tidal stream energy in China." *Procedia Engineering* 1 (16): 880–887. <https://doi.org/10.1016/j.proeng.2015.08.377>